Simulations of Photopumping in Doubly Illuminated Liquid Membranes Containing Photoactive Carriers

ARTICLE *in* THE JOURNAL OF PHYSICAL CHEMISTRY B · NOVEMBER 2010

Impact Factor: 3.3 · DOI: 10.1021/jp106802q · Source: PubMed

3 AUTHORS, INCLUDING:

Teresa Longin
University of Redlands
11 PUBLICATIONS **292** CITATIONS
SEE PROFILE

John Terhorst
Vanguard University
2 PUBLICATIONS **12** CITATIONS
SEE PROFILE

Simulations of Photopumping in Doubly Illuminated Liquid Membranes Containing Photoactive Carriers

Teresa L. Longin,* John Terhorst, and Christopher Lang

University of Redlands, 1200 East Colton Avenue, Redlands, California 92373-0999, United States

Received: July 21, 2010; Revised Manuscript Received: October 7, 2010

A steady-state model used to simulate photofacilitated active transport against a concentration gradient, called photopumping, is described. Central to this model is the idea that the carrier can be in either a strongly binding or a weakly binding form and light can be used to control the interconversion rate between the two forms. Most experimental and theoretical studies have focused on systems in which only one side of the membrane is illuminated at a time to form singly illuminated liquid membranes. This study explores membranes in which both the feed and the sweep side are illuminated simultaneously with light of different wavelengths to form doubly illuminated liquid membranes. Doubly illuminated liquid membranes can sustain transport against concentration gradients in which the solute concentration in the sweep is a factor of 10 or more higher than that in the feed, while transport in singly illuminated liquid membranes falls off at lower concentration gradients. In addition, carrier properties that are important in single illumination such as the interconversion rates between the weakly and the strongly binding forms of the carrier are not important for doubly illuminated membranes, meaning that the range of suitable carriers will be much greater for double illumination than for single illumination.

Introduction

For decades, chemists have been studying bulk liquid membrane systems which have the capacity to separate, purify, and concentrate solute in a relatively simple, efficient, and low-energy manner.[1−6] In a typical liquid membrane system (in contrast to a biomembrane or synthetic bilayer membrane), two batch solutions are separated by a thin immiscible liquid membrane. One of the batch solutions, called the *feed*, is enriched in a solute of interest, while the other, called the *sweep*, is dilute. Within the membrane are molecules called carriers that bind selectively and reversibly to the solute of interest. In general, the carriers are completely soluble in the membrane but completely insoluble in the batch solutions, while the solute is highly soluble in the batch solutions and sparingly soluble in the membrane solvent so that unfacilitated diffusion of the solute is very low.

The solute diffuses out of the highly concentrated feed solution into the membrane, where it complexes with the carrier to form a carrier−solute complex. As a sufficiently high concentration of the complex begins to build up along the feed−membrane interface, the complex begins to diffuse across the membrane toward the sweep−membrane interface, where it releases the solute. As solute is released at the sweep−membrane interface, the concentration gradient between the membrane and the sweep phase will allow the solute to diffuse into the dilute sweep solution. Eventually, uncomplexed carrier will accumulate at the sweep−membrane interface and begin to diffuse back toward the feed−membrane interface, where it will be able to bind to more solute, thus continuing transport and separation. While these membranes can be very selective for solute, they do not allow for transport against a concentration gradient between the feed and sweep solutions.

In 1977, Schultz proposed a more advanced membrane system that utilized light in a process known as photofacilitation.[7] Photofacilitated membranes contain carriers that are said to be *photoactive* in that light can drive conversion of the carriers into different physical configurations, allowing the solute to bind either strongly or weakly. Typically, either the feed side is illuminated to convert most of the weakly binding form of the carrier into the strongly binding form and enhance uptake of solute or the sweep side is illuminated to convert the strongly binding form of the carrier into the weakly binding form and promote release of the solute.[8−20] Several different chemically independent concentration gradients for individual species are simultaneously present within the membrane, and the concentration of solute inside the membrane at the sweep interface can become significantly greater than that in the bulk sweep solution. This allows for net transport of solute across the membrane even if the concentration of solute in the sweep solution is equal to or greater than that in the feed solution. Thus, photofacilitated membranes allow transport against an overall solute concentration gradient, called *photopumping*, which is particularly beneficial to those who wish to go beyond mere separation and concentrate solute for more efficient storage. Essentially, light energy is used to drive solute transport against a concentration gradient, allowing for purification and concentration of a particular component of a mixture. Several theoretical and experimental studies have demonstrated the feasibility of photopumping under single illumination,[15−21] and theoretical studies have provided information on what carrier and membrane properties should provide high levels of solute transport against a concentration gradient.[20,21]

Many potential photoactive carriers are photoactive in both forms, with each form absorbing light at different wavelengths.[8−14,17] This leads to the potential for doubly illuminated liquid membranes, and a few researchers have explored such membrane systems, both for photomodulation of transport rates[22−24] and for photopumping.[24] However, the wide range of

* To whom correspondence should be addressed. E-mail: Teresa_Longin@redlands.edu.

10.1021/jp106802q
Published on Web 11/11/2010

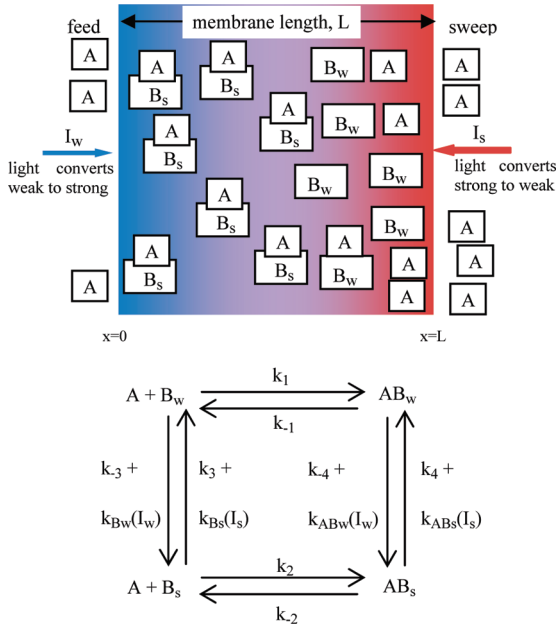

Figure 1. Schematic depiction of a doubly illuminated photofacilitated liquid membrane and the reaction scheme used as the model for photopumping. Light impinging on the feed interface converts the weakly binding form of the carrier (B_w) to the strongly binding form (B_s), which binds to the solute of interest (A) to form the strongly bound form of the carrier−solute complex (AB_s). The complex diffuses to the sweep interface where light of a different wavelength converts the complex to the weakly bound form (AB_w) which decomplexes, releasing free solute.

binding constants, interconversion rates between the strongly and the weakly binding forms, and other membrane properties used suggest a need for a more complete understanding of the factors important in photopumping.

Figure 1 depicts the model for photofacilitated transport leading to photopumping under double illumination used in this study. In this model, the carrier can exist in four forms: a strongly binding form (B_s), a weakly binding form (B_w), the strongly bound form of the carrier−solute complex (AB_s), and the weakly bound form of the carrier−solute complex (AB_w). The feed interface of the membrane is illuminated with light of the appropriate wavelength to convert B_w to B_s, which then complexes with free solute A to form the strongly bound form of the carrier−solute complex. This complex then diffuses to the sweep side of the membrane, which is illuminated with light of the proper wavelength to convert B_s to B_w, which results in conversion of the strongly bound form of the complex to the weakly bound form. Equilibrium favors dissociation of the complex, resulting in a high concentration of free solute, which then partitions into the sweep phase. This model is an extension of one developed for simulating solute transport and photopumping under single illumination,[20,21] and experimental testing of that model shows reasonable agreement with theoretical predictions.[13] Table 1 lists the parameters used in this manuscript.

In this study, we simulated transport in membranes where both sides of the membrane are illuminated simultaneously with light of different wavelengths. Such doubly illuminated membranes should show enhanced solute transport against a concentration gradient over singly illuminated membranes. This study explored which carrier and membrane properties (such as interconversion rates, complexation and decomplexation rates, carrier mobility, and photon absorption) most affect photopumping and what the optimal values of those properties are. Simulations were performed under two independent conditions: first, with the carrier primarily in the weakly binding form in the dark, and then with the carrier primarily in the strongly binding form in the dark.

Model

This model focuses on the membrane itself and does not consider the bulk feed or sweep solutions. When referring to either the feed or the sweep interface, the model considers the membrane side of the interface only, rather than the feed or sweep solution side of the interface. Hence, considerations such as partition coefficients, the rate of solute transfer across the interface, and diffusion within the bulk feed and sweep solutions are not included in the model. The total steady-state solute flux for particular membrane and carrier properties is determined using Fick's first law of diffusion:

$$J_A = -D_A\frac{d[A]}{dx} - D_{AB}\frac{d[AB_w]}{dx} - D_{AB}\frac{d[AB_s]}{dx} \quad (1)$$

In order to calculate the total solute flux, the concentration profiles across the membrane for the solute and each form of the carrier and carrier−solute complex must also be determined. These profiles are controlled by the reaction kinetics depicted in Figure 1 as well as by steady-state diffusion. The equations describing the steady-state concentration profiles for each species are given by Fick's second law of diffusion and are defined in a previous publication.[25] The equations are also included in the Supporting Information. The light intensity profiles are calculated using the Beer−Lambert law in its differential form as described in a previous publication[25] and are described in the Supporting Information. These equations do not contain any expressions for a thermal gradient and hence apply only to membranes maintained at a constant temperature which can be achieved in practice by filtering out undesired wavelengths of light to limit heating and keeping the membrane system in a cooled bath. It should also be noted that ionic effects were neglected since ionic solutes partition into the membrane in the form of ion pairs which maintain electroneutrality. Hence, the Nernst−Planck term is zero, and Fick's laws of diffusion are sufficient to describe the system.[26,27]

All concentrations, rate constants, and other parameters are made dimensionless in order to generalize the model and allow the application of results to a wide variety of membrane systems. The characteristics of a specific carrier and transport system can be compared to the generalized, optimal parameters to predict how effective the specific system should be at photopumping.

The concentration of the solute at any point across the membrane is normalized by the concentration of the solute inside the membrane at the feed interface, $[A]_o$. The concentration of each form of the carrier or carrier−solute complex is normalized by the total carrier concentration, C_T. The value of the position at any point across the membrane, x, is normalized by the membrane length, L, and denoted χ.

$$\bar{A} = \frac{[A]}{[A]_o}, \bar{B}_w = \frac{[B_w]}{C_T}, \bar{B}_s = \frac{[\bar{B}_s]}{C_T}, \overline{AB}_w = \frac{[AB_w]}{C_T}, \overline{AB}_s = \frac{[AB_s]}{C_T}, \chi = \frac{x}{L} \quad (2)$$

TABLE 1: List of Parameters Used in This Manuscript

parameter	definition	description	eqn
k_1		rate constant for complexation for the weak form of the carrier	
k_{-1}		rate constant for decomplexation for the weak form of the complex	
k_2		rate constant for complexation for the strong form of the carrier	
k_{-2}		rate constant for decomplexation for the strong form of the complex	
k_3		rate constant for thermal conversion of the strong form of the carrier to the weak form	
k_{-3}		rate constant for thermal conversion of the weak form of the carrier to the strong form	
k_4		rate constant for thermal conversion of the strong form of the complex to the weak form	
k_{-4}		rate constant for thermal conversion of the weak form of the complex to the strong form	
k_{B_w}		light intensity dependent rate constant for the conversion of weak form of carrier to strong form	
k_{AB_w}		light-intensity-dependent rate constant for conversion of the weak form of the complex to the strong form	
k_{B_s}		light-intensity-dependent rate constant for conversion of the strong form of the carrier to the weak form	
k_{AB_s}		light-intensity-dependent rate constant for conversion of the strong form of the complex to the weak form	
I_w		intensity of light of wavelength that converts the weak form of the carrier and complex to the strong form	
I_s		intensity of light of wavelength that converts the strong form of the carrier and complex to the weak form	
$[A]_o$		concentration of solute at the feed interface	
$[A]_L$		concentration of solute at the sweep interface	
C_T		total concentration of solute	
$\bar{A}$	$[A]/[A]_o$	normalized concentration of free solute in the membrane	2
$\bar{B}_w$	$[B_w]/C_T$	normalized concentration of the weak form of the carrier in the membrane	2
$\bar{B}_s$	$[B_s]/C_T$	normalized concentration of the strong form of the carrier in the membrane	2
$\overline{AB_w}$	$[AB_w]/C_T$	normalized concentration of the weak form of the complex in the membrane	2
$\overline{AB_s}$	$[AB_s]/C_T$	normalized concentration of the strong form of the complex in the membrane	2
χ	x/L	normalized distance across the membrane	2
$\bar{A}_L$	$[A]_L/[A]_o$	concentration gradient across the membrane	3
K_w	k_1/k_{-1}	binding constant for the weak form of the carrier	4
K_s	k_2/k_{-2}	binding constant for the strong form of the carrier	5
K_w^d	$(k_1/k_{-1})[A]_o$	dimensionless binding constant for the weak form of the carrier	6
K_s^d	$(k_2/k_{-2})[A]_o$	dimensionless binding constant for the strong form of the carrier	6
K_{car_o}	k_3/k_{-3}	thermal equilibrium constant between the strong and the weak forms of the carrier	7
K_{com_o}	k_4/k_{-4}	thermal equilibrium constant between the strong and the weak forms of the complex	8
$K_{car}(I)$	$(k_3 + k_{B_w})/(k_{-3} + k_{B_s})$	light-intensity-dependent equilibrium constant between the strong and the weak forms of the carrier	7
$K_{com}(I)$	$(k_4 + k_{AB_w})/(k_{-4} + k_{AB_s})$	light-intensity-dependent equilibrium constant between the strong and the weak forms of the complex	8
ε_w	$D_{AB}/(L^2k_{-1})$	parameter containing rate constant for decomplexation of the weak form of the complex	15
ε_s	$D_{AB}/(L^2k_{-2})$	parameter containing rate constant for decomplexation of the strong form of the complex	15
ε_{car_o}	$D_{AB}/(L^2k_{-3})$	parameter containing rate constant for thermal conversion of the weak form of the carrier to the strong form	16
ε_{com_o}	$D_{AB}/(L^2k_{-4})$	parameter containing rate constant for thermal conversion of the weak form of the complex to the strong form	16
α	$D_{AB}C_T/D_A[A]_o$	mobility parameter	19
$\tilde{E}$		molar absorptivity coefficient in units of L/mol cm	
$\beta_{car,w}$	$\tilde{E}_{B_w}C_TLZ$	normalized molar absorptivity coefficient for the weak form of the carrier	20
$\beta_{car,s}$	$\tilde{E}_{B_s}C_TL$	normalized molar absorptivity coefficient for strong form of carrier	20
$\beta_{com,w}$	$\tilde{E}_{AB_w}C_TL$	normalized molar absorptivity coefficient for the weak form of the complex	21
$\beta_{com,s}$	$\tilde{E}_{AB_s}C_TL$	normalized molar absorptivity coefficient for the strong form of the complex	21

Of particular interest to this study is the value of the solute concentration inside the membrane at the sweep interface, $[A]_L$, since the goal of this study is to explore the change in solute flux as the solute concentration at the sweep interface increases relative to the solute concentration at the feed interface. This concentration gradient is defined as

$$\bar{A}_L = \frac{[A]_L}{[A]_o} \tag{3}$$

This value is referred to as the normalized [A] in sweep in subsequent figures.

The binding constants for the strongly and weakly binding forms of the carrier−solute complex are defined by the binding equilibrium equations:

$$A + B_w \underset{k_{-1}}{\overset{k_1}{\rightleftharpoons}} AB_w \quad K_w = \frac{k_1}{k_{-1}} \tag{4}$$

$$A + B_s \underset{k_{-2}}{\overset{k_2}{\rightleftharpoons}} AB_s \quad K_s = \frac{k_2}{k_{-2}} \tag{5}$$

The binding constants are made dimensionless by correcting for the concentration of the solute at the feed interface:

$$K_w^d = \frac{k_1}{k_{-1}}[A]_o, \quad K_s^d = \frac{k_2}{k_{-2}}[A]_o \tag{6}$$

The rate constants for complexation and decomplexation are temperature dependent but not impacted by light and so will be referred to as being purely thermal. The binding equilibrium constants depend on the rate constants and are also purely thermal.

In contrast, rate constants for interconversion between the weakly and strongly binding forms of the carrier and the carrier−solute complex have both a purely thermal and a light-intensity-dependent component. Consequently, the equilibrium constants also have both a purely thermal and a light-intensity-dependent form, as shown in eqs 7 and 8

$$B_s \underset{k_{-3} + k_{B_w}(I_w)}{\overset{k_3 + k_{B_s}(I_s)}{\rightleftharpoons}} B_w \quad K_{car_o} = \frac{k_3}{k_{-3}} = \frac{[B_w]}{B_s}$$

$$K_{car}(I) = \frac{k_3 + k_{B_w}(I_s)}{k_{-3} + k_{B_s}(I_w)} \tag{7}$$

$$AB_s \underset{k_{-4} + k_{AB_w}(I_w)}{\overset{k_4 + k_{AB_s}(I_s)}{\rightleftharpoons}} AB_w \quad K_{como} = \frac{k_4}{k_{-4}} = \frac{[AB_w]}{[AB_s]}$$

$$K_{com}(I) = \frac{k_4 + k_{AB_w}(I_s)}{k_{-4} + k_{AB_s}(I_w)} \tag{8}$$

I_s is the intensity of the light of the appropriate wavelength to convert the strongly binding form of the carrier to the weakly binding form, while I_w is the intensity of the light that converts the weakly binding form to the strongly binding form. The term K_{caro} applies to the thermal or "dark" equilibrium constant between the weakly and the strongly binding forms of the carrier, while K_{como} refers to the thermal equilibrium constant between the two forms of the carrier−solute complex. $K_{car}(I)$ and $K_{com}(I)$ are the light-intensity-dependent equilibrium constants for the equilibria between the weakly and the strongly binding forms of the carrier and carrier−solute complex, respectively. In this model, the light intensity affects the rate constants for interconversion between the strongly and the weakly binding forms of the carrier and complex and so affects the relative concentrations of each form.

Light intensities are incorporated into dimensionless parameters in the form of ratios of light-dependent rate constants to the thermal rate constants for interconversion between the forms of the carrier and complex. These ratios are denoted as η_{car} and η_{com}.

$$\eta_{car,s} = \frac{\Phi_{B_s} E_{B_s} I_{o,s}}{k_3} \tag{9}$$

$$\eta_{car,w} = \frac{\Phi_{B_w} E_{B_w} I_{o,w}}{k_{-3}} \tag{10}$$

$$\eta_{com,s} = \frac{\Phi_{AB_s} E_{AB_s} I_{o,s}}{k_4} \tag{11}$$

$$\eta_{com,w} = \frac{\Phi_{AB_w} E_{AB_w} I_{o,w}}{k_{-4}} \tag{12}$$

In these parameters, Φ is the quantum yield for light absorption by the carrier and E is the molar absorptivity coefficient for the carrier in units of cm^2/mol. $I_{o,s}$ is the incident value of I_s at the feed interface, while $I_{o,w}$ is the incident value of I_w at the sweep interface. Incorporating these parameters into the light-intensity-dependent expressions for the equilibrium constants between the weakly and the strongly binding forms of the carrier and complex yields

$$K_{car}(I) = K_{car_o}\left(\frac{1 + \eta_{car,s}\bar{I}_s}{1 + \eta_{car,w}\bar{I}_w}\right) \tag{13}$$

$$K_{com}(I) = K_{com_o}\left(\frac{1 + \eta_{com,s}\bar{I}_s}{1 + \eta_{com,w}\bar{I}_w}\right) \tag{14}$$

Previous theoretical studies of liquid membranes have indicated that the rate constants for decomplexation of the carrier−solute complex play a significant role in the flux of solute across the membrane.[6,19,20,25] These rate constants are incorporated into dimensionless parameters using the diffusion coefficient for the carrier−solute complex, D_{AB}, and the membrane length, L.

$$\varepsilon_w = \frac{D_{AB}}{L^2 k_{-1}} \text{ and } \varepsilon_s = \frac{D_{AB}}{L^2 k_{-2}} \tag{15}$$

The parameters ε_s and ε_w relate decomplexation reaction times to diffusion times, and small values of the parameters indicate large decomplexation rate constants and fast reaction times. Note that the carrier is assumed to be significantly larger than the solute, so the diffusion coefficients for the carrier and the complex are approximately the same and given by D_{AB}. This assumption has been used in a number of previous theoretical studies of facilitated transport in liquid membranes[6,19,20,24] and applies to most of the carriers and solutes in the cited transport studies.

The dimensionless parameters involving the rate constants for interconversion between forms of the carrier and complex also relate the rate constants to D_{AB} and L. The purely thermal, "dark" parameters are defined as

$$\varepsilon_{car_o} = \frac{D_{AB}}{L^2 k_{-3}} \text{ and } \varepsilon_{com_o} = \frac{D_{AB}}{L^2 k_{-4}} \tag{16}$$

The parameters incorporating light become

$$\varepsilon_{car}(I) = \frac{D_{AB}}{L^2(k_{-3} + k_{B_s}(I_s))} = \frac{\varepsilon_{car_o}}{1 + \eta_{car,s}\bar{I}_s} \quad (17)$$

$$\varepsilon_{com}(I) = \frac{D_{AB}}{L^2(k_{-4} + k_{AB_s}(I_s))} = \frac{\varepsilon_{com_o}}{1 + \eta_{com,s}\bar{I}_s} \quad (18)$$

Additional important characteristics of the membrane and carrier are the relative mobilities of the carrier and solute and the molar absorptivity coefficient of the carrier. The mobility of the carrier is related to the mobility of the solute through the mobility parameter, α.

$$\alpha = \frac{D_{AB}C_T}{D_A A_o} \quad (19)$$

The dimensionless molar absorptivity coefficients for each form of the carrier and complex are defined as

$$\beta_{car,w} = \tilde{E}_{B_w}C_T L, \beta_{car,s} = \tilde{E}_{B_s}C_T L \quad (20)$$

$$\beta_{com,w} = \tilde{E}_{AB_w}C_T L, \beta_{com,s} = \tilde{E}_{AB_s}C_T L \quad (21)$$

$\tilde{E}$ is the molar absorptivity coefficient in units of L/mol cm.

Simulation Methodology

In order to determine the solute flux under a given set of carrier and membrane properties, the FORTRAN program BVPFD was used to solve the mass transport and light intensity equations for all species in the membrane, as described in a previous publication.[25] The text for the program (called "doublefiatluxweak") used for the simulations is provided in the Supporting Information. The higher the solute flux value the better the transport across the membrane. For the simulations done in these experiments, a given variable was changed and the rest were held constant to determine the highest flux values under both single and double illumination. For example, in order to determine the impact of the equilibrium constants between the weakly and the strongly binding forms of the carrier and complex, K_{caro} and K_{como} were changed systematically while K^d_s, K^d_w, $\beta_{car,w}$, $\beta_{car,s}$, $\beta_{com,w}$, $\beta_{com,s}$, α, ε_{caro}, and ε_{como} were kept constant.

For each set of constants, the solute concentration gradient $\bar{A}_L$ was initially set to zero, that is, the solute concentration at the sweep interface was set to zero relative to the solute concentration at the feed interface. To simulate single illumination, the light intensity impinging on either the feed interface (for carriers with $K_{caro} > 1$) or the sweep interface (for carriers with $K_{caro} < 1$) was gradually increased while the light intensity at the opposite interface was kept at zero until a light intensity was reached that provided maximum solute transport. This was recorded as the optimal flux under single illumination. The light intensity at the opposite interface was then gradually increased until a maximum flux was obtained. The light intensity at the original interface was then gradually increased until a new maximum flux was obtained. This process was repeated until there was no significant increase in the flux with increasing light intensity. The concentration gradient was then set to one, and the process was repeated to obtain a maximum flux under both single and double illumination. This process was continued up to a concentration gradient of 10.

The program BVPFD was used because it uses Newton's method to solve a series of differential equations with boundary conditions at two points for each equation. It allows the use of a logarithmic χ grid, providing points very close together at the edges of the membrane where the concentrations change rapidly and further apart toward the center of the membrane where the concentrations do not change as rapidly. If necessary, the program will automatically add more χ points in order to achieve convergence. For the series of simulations described in this paper, the number of χ points used for the initial guess was typically 151. If necessary, the results of a previous simulation could be used as an initial guess; the text of the program (called "translate") used to convert results into an initial guess is provided in the Supporting Information. This subroutine has been used in previous studies to solve similar equations.[20,21,25]

Results and Discussion

In order to investigate the benefits of double illumination over single illumination, we chose to separate the simulations into two parts. Realistically, a potential carrier will predominantly be in the weakly binding form in the dark, will predominantly be in the strongly binding form in the dark, or will have an equal concentration of the two forms. We first explored simulated transport for carriers that predominately exist as the weakly binding form in the dark ($[B_w]/[B_s] > 1$) then looked at the case in which the carrier is predominantly in the strongly binding form in the dark ($[B_w]/[B_s] < 1$). The central focus of these investigations was to determine whether double illumination provided better solute transport against a concentration gradient than single illumination and what carrier and membrane properties would make double illumination of the membrane most beneficial.

Results for Simulations in Which the Carrier Is Predominantly in the Weakly Binding Form in the Dark. ***Effects of the Equilibrium Constant between the Weakly and Strongly Binding Forms of the Carrier.*** Simulations were run determining the dimensionless solute flux at various normalized solute concentrations in the sweep phase while varying the equilibrium constant between the weakly and strongly binding forms of the carrier in the dark (K_{caro}), which is defined in eq 7. The equilibrium constant between the strongly and the weakly binding forms of the bound carrier−solute complex (K_{como}) depends on K_{caro}, so it was not necessary to vary that parameter separately. Results are shown in Figure 2. Under single illumination (Figure 2a), the ability of the membrane to maintain active transport against a concentration gradient rapidly decreases as the equilibrium constant between the weakly and the strongly binding forms of the carrier decreases, which is consistent with previously published results.[19,20] This indicates that in order to maintain high solute transport rates against significant concentration gradients, the weakly binding form of the carrier must be strongly favored thermodynamically. In contrast, under double illumination (see Figure 2b), the value of K_{caro} has no effect on the solute flux at any concentration gradient. Furthermore, solute transport is significantly higher under double illumination for all values of K_{caro}, particularly at high concentration gradients.

Double illumination provides two benefits. First, carriers that are optimal for photopumping under single illumination will provide even better performance under double illumination. Second, carriers with other optimal characteristics but with too small a value of K_{caro} to perform well under single illumination

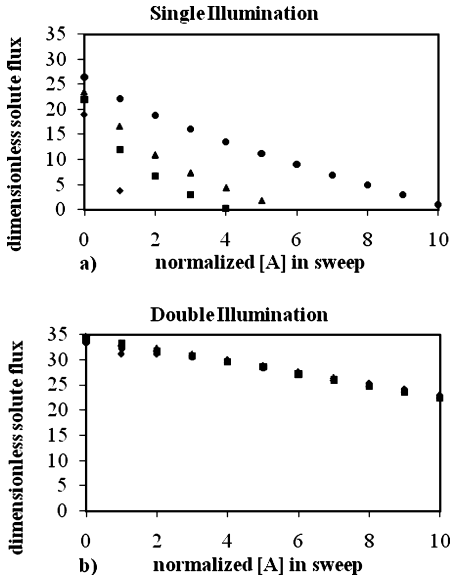

Figure 2. Plots of dimensionless solute flux versus the normalized concentration of solute in the sweep solution as a function of K_{caro}, which is the thermal equilibrium constant between the strongly and weakly binding forms of the carrier. The carrier is predominantly in the weakly binding form in the dark, and $K^d_s = 5$, $K^d_w = 0.005$, $\alpha = 50$, $\beta_{car,w} = \beta_{car,s} = \beta_{com,w} = \beta_{com,s} = 10$, $\varepsilon_{caro} = \varepsilon_{como} = 1$, and $\varepsilon_s = \varepsilon_w = 0.01$. (a) Plots of the dimensionless solute flux versus solute concentration gradient under single illumination: (♦) $K_{caro} = 10$; (■) $K_{caro} = 50$; (▲) $K_{caro} = 100$; (●) $K_{caro} = 500$. (b) Plots of the dimensionless solute flux versus solute concentration under double illumination: (♦) $K_{caro} = 10$; (■) $K_{caro} = 50$; (▲) $K_{caro} = 100$; (●) $K_{caro} = 500$. Under single illumination, transport strongly depends on the value of the thermal equilibrium constant between the strongly and the weakly binding forms of the carrier. Under double illumination, flux against a given concentration gradient is greater than under single illumination and is independent of the equilibrium constant.

should provide significant photopumping under double illumination, increasing the pool of potential photocarriers.

The mechanism for greater flux under double illumination than under single illumination is illustrated in Figure 3. Figure 3a shows plots of normalized solute concentrations across the membrane under single and double illumination at optimal light intensities. Under double illumination, the solute concentration gradients at the feed and sweep interfaces are much steeper than they are under single illumination, leading to higher solute flux under double illumination.

The solute concentration profiles are in turn explained by the carrier concentration profiles shown in Figure 3b and 3c. The total normalized concentrations of the strongly binding forms of the carrier and carrier−solute complex are much greater at the feed interface under double illumination than under single illumination, as shown in Figure 3b. This means that much more solute can be drawn into the membrane under double illumination than under single illumination. Conversely, the total normalized concentrations of the weakly binding forms of the carrier and complex are much higher at the sweep interface under double illumination than under single illumination as shown in Figure 3c. This means that there will be high concentrations of free solute at the sweep interface under double illumination, which means higher flux of solute out of the membrane. Under double illumination, a high intensity of the wavelength of light needed to convert the weakly binding form of the carrier to the strongly binding form can be used at the feed interface in order to convert most of the weakly binding form to the strongly binding form, while light impinging on

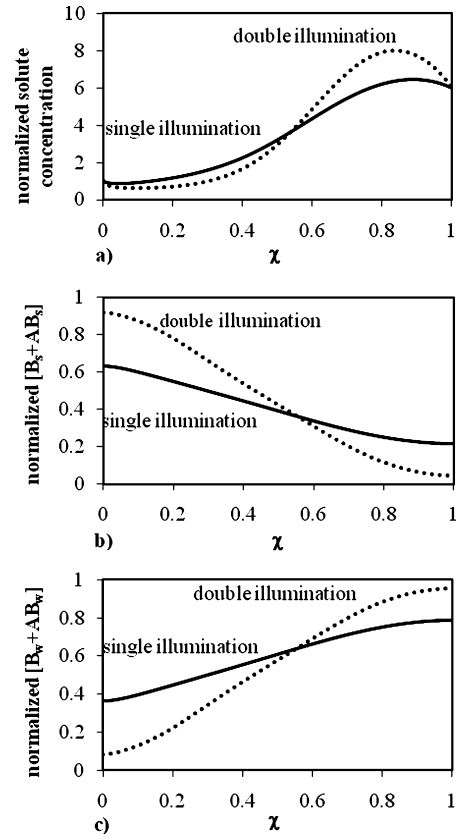

Figure 3. Plots of normalized solute and carrier concentrations across the membrane during optimal conditions for photopumping. The carrier is predominantly in the weakly binding form in the dark, and $K^d_s = 5$, $K^d_w = 0.005$, $K_{caro} = 500$, $\varepsilon_{caro} = \varepsilon_{como} = 1$, $\alpha = 50$, $\beta_{car,w} = \beta_{car,s} = \beta_{com,w} = \beta_{com,s} = 10$, and $\varepsilon_s = \varepsilon_w = 0.01$. (a) Plots of normalized solute concentrations across the membrane under single and double illumination. (b) Plots of the total normalized concentrations of the strongly binding forms of the carrier and complex across the membrane under single and double illumination. (c) Plots of the total normalized concentrations of the weakly binding forms of the carrier and complex across the membrane under single and double illumination.

the sweep interface converts the strongly binding form back to the weakly binding form. Under single illumination, use of such a high light intensity at the feed interface would photobleach the membrane and convert most of the carrier to the strongly binding form across the membrane, reducing the concentration of free solute at the sweep interface and consequently reducing solute flux. A value of 500 was chosen for K_{caro} for testing further parameters, since that value provided good photopumping under both single and double illumination.

Effects of Interconversion Rate Constants between the Weakly and Strongly Binding Forms of the Carrier. The rate constants for interconversion between the strongly and the weakly binding forms of the carrier and complex are contained in the parameters ε_{caro} and ε_{como}, defined in eq 16. As shown in this equation, ε_{caro} and ε_{como} are inversely proportional to the interconversion rate constants, so small values of ε_{caro} and ε_{como} represent large interconversion rate constants. Figure 4 shows the results for simulations of solute transport against a concentration gradient as a function of ε_{caro} and ε_{como}. Under single illumination (Figure 4a), the ability of the membrane to transport solute against a concentration gradient improved as the values of ε_{caro} and ε_{como} decreased to 0.1 and then remained constant. This indicates that under single illumination, the carrier should have fairly large interconversion rate constants in order to provide good photopumping performance, as shown in previous

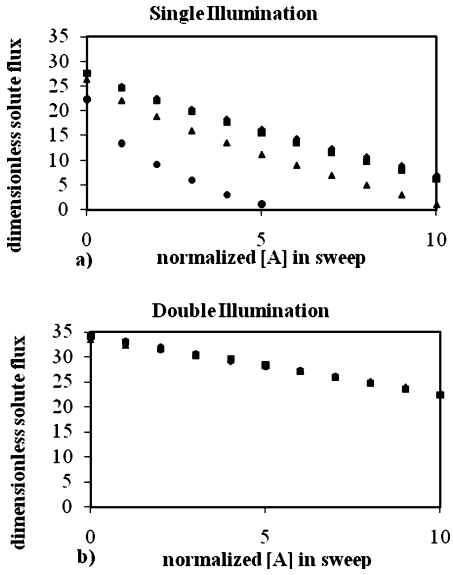

Figure 4. Plots of dimensionless solute flux versus the normalized concentration of solute in the sweep solution as a function ε_{caro} and ε_{como}. These parameters are inversely proportional to the thermal rate constant for conversion between the strongly and the weakly binding forms of the carrier and complex so that as the rate constants increase ε_{caro} and ε_{como} decrease. The carrier is predominantly in the weakly binding form in the dark, and $K^d_s = 5$, $K^d_w = 0.005$, $K_{caro} = 500$, $\alpha = 50$, $\beta_{car,w} = \beta_{car,s} = \beta_{com,w} = \beta_{com,s} = 10$, and $\varepsilon_s = \varepsilon_w = 0.01$. (a) Plots of the dimensionless solute flux versus solute concentration under single illumination: (♦) $\varepsilon_{caro} = \varepsilon_{como} = 0.01$; (■) $\varepsilon_{caro} = \varepsilon_{como} = 0.1$; (▲) $\varepsilon_{caro} = \varepsilon_{como} = 1$; (●) $\varepsilon_{caro} = \varepsilon_{como} = 10$. (b) Plots of the dimensionless solute flux versus solute concentration under double illumination: (♦) $\varepsilon_{caro} = \varepsilon_{como} = 0.01$; (■) $\varepsilon_{caro} = \varepsilon_{como} = 0.1$; (▲) $\varepsilon_{caro} = \varepsilon_{como} = 1$; (●) $\varepsilon_{caro} = \varepsilon_{como} = 10$. Under single illumination, as ε_{car} and ε_{com} increase (meaning the interconversion rate constants decrease) transport rapidly declines as the concentration gradient increases. For double illumination, the magnitudes of ε_{car} and ε_{com} have no effect on solute flux, meaning that the magnitudes of interconversion rate constants have no effect on solute flux.

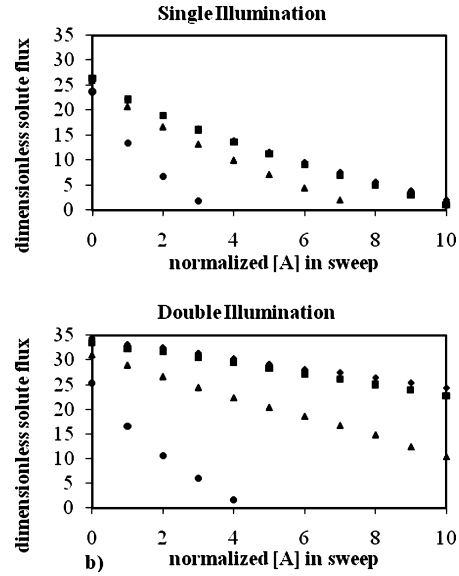

Figure 5. Plots of dimensionless solute flux versus the normalized concentration of solute in the sweep solution as a function of the binding constant for the weakly binding form of the carrier, K^d_w. The carrier is predominantly in the weakly binding form in the dark, and $K^d_s = 5$, $K_{caro} = 500$, $\varepsilon_{caro} = \varepsilon_{como} = 1$, $\alpha = 50$, $\beta_{car,w} = \beta_{car,s} = \beta_{com,w} = \beta_{com,s} = 10$, and $\varepsilon_s = \varepsilon_w = 0.01$. (a) Plots of the dimensionless solute flux versus normalized solute concentration in the sweep solution under single illumination: (♦) $K^d_w = 0.0005$; (■) $K^d_w = 0.005$; (▲) $K^d_w = 0.05$; (●) $K^d_w = 0.5$. (b) Plots of the dimensionless solute flux versus solute concentration under double illumination: (♦) $K^d_w = 0.0005$; (■) $K^d_w = 0.005$; (▲) $K^d_w = 0.05$; (●) $K^d_w = 0.5$. Under both single and double illumination, transport improves significantly as K^d_w decreases from 0.5 to 0.005; further decreases in K^d_w do not improve transport. As with other simulations, double illumination produces significantly higher flux than single illumination, especially at high concentration gradients and optimal values of K^d_w.

work.[19,20] If the rate constant for interconversion is low, then the carrier stays in the strongly binding form of the carrier for a relatively long time, meaning significant amounts will still be in the strongly binding form when the carrier−solute complex reaches the sweep interface, so decomplexation does not occur close to the interface. This means less free solute in the membrane that can diffuse into the sweep phase, which results in a lower solute flux.

Conversely, under double illumination, the values of ε_{caro} and ε_{como} have no impact on the photopumping ability of the membrane, as shown in Figure 4b. In addition, double illumination results in higher transport rates than single illumination, even for large interconversion rate constants. The use of light at the sweep interface rapidly converts the strongly bound form of the complex to the weakly bound form, resulting in more decomplexation and higher levels of free solute at the sweep interface than under single illumination. Consequently, it does not matter whether interconversion kinetics are fast or slow; illumination overcomes any thermal limitations. A carrier that might have interconversion rate constants that are too low to be optimal under single illumination could be a good carrier under double illumination, if its other characteristics are optimal. As with K_{caro} and K_{como}, this means that the potential pool of carriers for double illumination is greater than that for single illumination.

A value of 1 was chosen for ε_{caro} and ε_{como} for testing the remaining parameters. That value provided good performance under both single and double illumination, and the program easily reached convergence at that value under most conditions.

Effects of the Binding Constants K^d_s and K^d_w. Exploring the effects of the binding constants (defined in eq 6) separately from each other poses some challenges. Changing the binding constant for the strongly binding form of the carrier (K^d_s) while keeping the binding constant for the weakly binding form of the carrier (K^d_w) the same will also change the ratio between the two, which could have an impact on transport separate from just the magnitudes of the binding constants. Alternatively, keeping the ratio between the constants the same while altering K^d_s means that K^d_w must also change, which is also likely to have an impact on membrane performance. We decided to first change the value of K^d_w while keeping the value of K^d_s at a moderate value of 5, since previous work had indicated that moderate values of K^d_s provide for high solute transport.[20,21,25]

Figure 5a shows the results of simulations for single illumination in which K^d_w were varied while the value of K^d_s was kept at 5. Membrane performance improved as the value of K^d_w decreased until it reached 0.005; then performance no longer improved. This indicates that low values of K^d_w are necessary to ensure that the weakly binding form of the carrier does not tie up significant amounts of the solute at the sweep interface. Figure 5b shows results of simulations under double illumination, and the behavior is qualitatively similar to that for single illumination, with the exception that transport against a concentration gradient was significantly higher under double illumination than under single illumination, consistent with previous trends noted in this study.

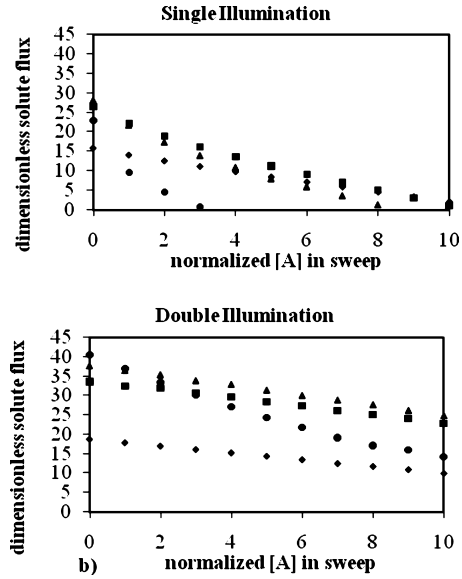

Figure 6. Plots of dimensionless solute flux versus the normalized concentration of solute in the sweep solution as a function of the binding constant for the strongly binding form of the carrier, K^d_s. For all cases, the carrier is predominantly in the weakly binding form in the dark, and $K^d_s/K^d_w = 1000$, $K_{caro} = 500$, $\varepsilon_{caro} = \varepsilon_{como} = 1$, $\alpha = 50$, $\beta_{car,w} = \beta_{car,s} = \beta_{com,w} = \beta_{com,s} = 10$, and $\varepsilon_s = \varepsilon_w = 0.01$. (a) Plots of the dimensionless solute flux versus solute concentration under single illumination: (♦) $K^d_s = 1$, $K^d_w = 0.001$; (■) $K^d_s = 5$, $K^d_w = 0.005$; (▲) $K^d_s = 10$, $K^d_w = 0.01$; (●) $K^d_s = 100$, $K^d_w = 0.1$. (b) Plots of the dimensionless solute flux versus solute concentration under double illumination: (♦) $K^d_s = 1$, $K^d_w = 0.001$; (■) $K^d_s = 5$, $K^d_w = 0.005$; (▲) $K^d_s = 10$, $K^d_w = 0.01$; (●) $K^d_s = 100$, $K^d_w = 0.1$. Under both single and double illumination, solute transport is greatest when K^d_s ranges from 1 to 10. However, double illumination produces significantly greater flux for all values of K^d_s, particularly when the sweep concentration of solute is at least a factor of 5 greater than the feed concentration.

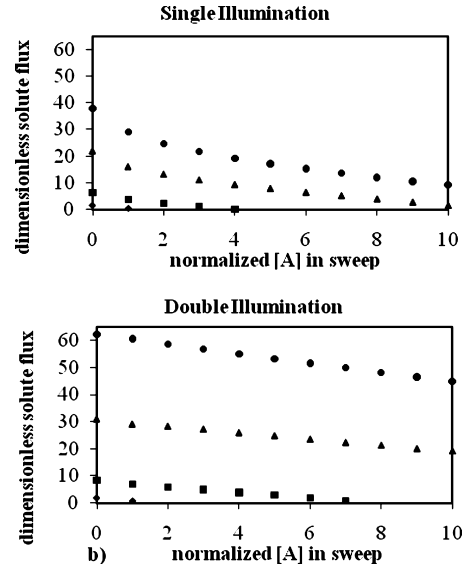

Figure 7. Plots of dimensionless solute flux versus the normalized concentration of solute in the sweep solution as a function of the ratio of carrier mobility to solute mobility contained in the parameter α. The carrier is predominantly in the weakly binding form in the dark, and $K^d_s = 5$, $K^d_w = 0.005$, $K_{caro} = 500$, $\varepsilon_{caro} = \varepsilon_{como} = 1$, $\beta_{car,w} = \beta_{car,s} = \beta_{com,w} = \beta_{com,s} = 10$, and $\varepsilon_s = \varepsilon_w = 0.01$. (a) Plots of the dimensionless solute flux versus solute concentration under single illumination: (♦) $\alpha = 1$; (■) $\alpha = 10$; (▲) $\alpha = 50$; (●) $\alpha = 100$. (b) Plots of the dimensionless solute flux versus solute concentration under double illumination: (♦) $\alpha = 1$; (■) $\alpha = 10$; (▲) $\alpha = 50$; (●) $\alpha = 100$. For both double and single illumination, solute flux increases as α increases but both the flux and the increase in flux are greater under double illumination.

In order to study the effect of K^d_s, the ratio between K^d_s and K^d_w was kept at 1000, since that ratio produced good results under both single and double illumination. Results of varying the values of K^d_s and K^d_w while maintaining a constant ratio between them are shown in Figure 6. Interestingly, the results for $K^d_s = 1$ and $K^d_w = 0.001$ are about the same under both single and double illumination. The value of K^d_w is low enough that the weak form of the carrier−solute complex will dissociate at the sweep interface. However, the value of K^d_s is too low to draw much solute into the membrane at the feed interface under either illumination condition, so double illumination provides little improvement in solute flux.

Under both double- and single-illumination conditions, optimum flux was seen with moderate values of K^d_s. When $K^d_s = 100$, flux fell off under both single and double illumination, although performance under double illumination was significantly better than under single illumination. This is an illustration of the advantage of double illumination. Under single illumination, a large value of K^d_s means that equilibrium will favor the strongly bound form of the carrier−solute complex in the presence of solute, even with a moderate value of K_{caro}. Under single illumination, light converts the weakly binding form to the strongly binding form, but since equilibrium favors the strongly bound form of the complex, not much of the complex converts to the weakly bound form at the sweep interface, so not much solute is released to diffuse into the sweep phase, resulting in low solute flux. Under double illumination, light on the sweep side forces the conversion of the strongly bound form of the carrier−solute complex to the weakly bound form, resulting in higher concentrations of free solute and relatively high solute flux.

For further simulations, $K^d_s = 5$ and $K^d_w = 0.005$ since that set of values provided good transport under both single and double illumination, allowing for easy comparison.

Effect of Carrier Mobility. The relative carrier mobility is contained in the parameter α as defined in eq 19. As the carrier mobility relative to solute mobility increases, α increases. Figure 7 shows the results for simulations of solute transport against a concentration gradient as α was varied from 1 to 100. Under both single and double illumination, transport increases significantly as α increases and values of α greater than 10 are necessary to maintain any sort of transport against a concentration gradient greater than a factor of 2. As with other parameters, transport in doubly illuminated membranes increases much more with increasing α than does transport in singly illuminated membranes. Clearly, it is essential to have a high carrier mobility for effective transport against a concentration gradient, which can be achieved by having a large carrier to solute concentration ratio at the feed interface.

Effect of Molar Absorptivity Coefficient for the Carrier. The molar absorptivity coefficients for the two forms of the carrier and complex are contained in the parameter β, defined in eqs 20 and 21, and are directly proportional to β. In order to study the effect of these parameters, values of β for all forms of the carrier and carrier−solute complex were set equal to each other. The implicit assumption is that the two forms of the carrier have similar molar absorptivity coefficients and that complexation does not affect the value of the molar absorptivity coefficient. This is to simplify the calculations and explore general trends related to the molar absorptivity coefficients. For specific carrier−solute systems, the molar absorptivity coefficients might be very different. In that case, the values for the

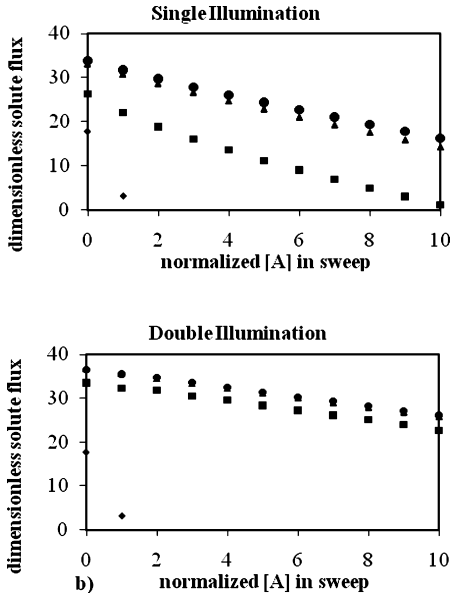

Figure 8. Plots of dimensionless solute flux versus the normalized concentration of solute in the sweep solution as a function of the parameter β. This parameter is a measure of the molar absorptivity of the carrier, and β increases as the molar absorptivity of the carrier increases. The carrier is predominantly in the weakly binding form in the dark, and $K^d_s = 5$, $K^d_w = 0.005$, $K_{caro} = 500$, $\varepsilon_{caro} = \varepsilon_{como} = 1$, $\alpha = 50$, and $\varepsilon_s = \varepsilon_w = 0.01$. (a) Plots of the dimensionless solute flux versus solute concentration under single illumination: (♦) all $\beta = 1$; (■) all $\beta = 10$; (▲) all $\beta = 50$; (●) all $\beta = 100$. (b) Plots of the dimensionless solute flux versus solute concentration under double illumination: (♦) all $\beta = 1$; (■) all $\beta = 10$; (▲) all $\beta = 50$; (●) all $\beta = 100$. For both double and single illumination, solute flux increases with β until β reaches 50, at which point increasing β fails to increase solute flux. Solute flux is greater under double illumination at high concentration gradients.

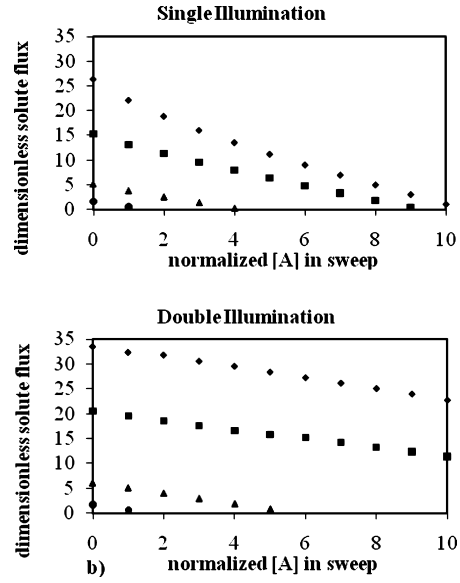

Figure 9. Plots of dimensionless solute flux versus the normalized concentration of solute in the sweep solution as a function of the parameters ε_s and ε_w. These parameters are measures of the dissociation rate constants for the solute/carrier complexes; as the rate constants increase, ε_s and ε_w decrease. For all cases, the carrier is predominantly in the weakly binding form in the dark and $K^d_s = 5$, $K^d_w = 0.005$, $K_{caro} = 500$, $\varepsilon_{caro} = \varepsilon_{como} = 1$, $\alpha = 50$, and $\beta_{car,w} = \beta_{car,s} = \beta_{com,w} = \beta_{com,s} = 10$. (a) Plots of the dimensionless solute flux versus solute concentration under single illumination: (♦) $\varepsilon_s = \varepsilon_w = 0.01$; (■) $\varepsilon_s = \varepsilon_w = 0.1$; (▲) $\varepsilon_s = \varepsilon_w = 1$; (●) $\varepsilon_s = \varepsilon_w = 10$. (b) Plots of the dimensionless solute flux versus solute concentration under double illumination: (♦) $\varepsilon_s = \varepsilon_w = 0.01$; (■) $\varepsilon_s = \varepsilon_w = 0.1$; (▲) $\varepsilon_s = \varepsilon_w = 1$; (●) $\varepsilon_s = \varepsilon_w = 10$. For both single and double illumination, solute transport falls off rapidly with increasing ε. However, for low values of ε and fast decomplexation rates, solute transport is significantly greater under double illumination than under single illumination.

carrier and complex would need to be experimentally determined and those specific values used in the model to predict results.

For both single- and double-illumination conditions, a relatively high value of β ($\beta \geq 10$) is necessary to maintain active transport, as shown in Figure 8. This makes sense since the light must be absorbed efficiently to have any impact on the transport rate. For singly illuminated membranes (Figure 8a), transport improves as β increases from 1 to 10 to 50; further increases in the value of β do not result in improved transport. For doubly illuminated membranes (Figure 8b), transport is about the same for values of β of 10 or greater. Again, double illumination produces higher transport than single illumination.

Effect of the Decomplexation Rate Constant for the Carrier−Solute Complex. The rate constants for decomplexation for the strongly and weakly bound forms of the carrier−solute complex are contained in the parameters ε_s and ε_w, respectively. These parameters are defined in eq 15, and the value of ε_s and ε_w are inversely proportional to the rate constants. Thus, as the decomplexation kinetics get faster, the values of ε_s and ε_w decrease. Figure 9 shows the results for simulations of photopumping as a function of a range of values of ε_s and ε_w for single and double illumination. For both doubly and singly illuminated membranes, relatively small values of ε_s and ε_w (meaning relatively large decomplexation rate constants) are needed to maintain photopumping. The carrier must be able to release the solute rapidly at the sweep interface or the build-up of free solute is insufficient to maintain the internal concentration gradient necessary to maintain fast transport against the feed−sweep concentration gradient. While double illumination provides faster transport for when decomplexation kinetics are fast, it cannot compensate for slow decomplexation kinetics.

Light Intensity. Double illumination requires much higher light intensities to maintain net solute transport against a concentration gradient than does single illumination. For carriers that are predominantly in the weakly binding form in the dark, only the feed side would be illuminated under single illumination. The light intensity on the feed side needed to achieve maximum solute flux at a given concentration gradient must be 5−10 times greater under double illumination than under single illumination. For double illumination, the light intensity on the sweep interface will be much lower than that on the feed interface, usually by a factor of 30 or more. However, while double illumination is more "expensive" than single illumination in terms of the number of photons required to achieve maximum flux, there are many carrier and membrane conditions under which double illumination will provide net solute transport against much higher concentration gradients than can single illumination. For example, for carriers with small interconversion rate constants, double illumination can maintain high solute flux against concentration gradients of a factor of 10 or greater, while single illumination can only maintain transport against gradients of 6 or less, as shown in Figure 2. For double illumination, optimal flux is attained when the light intensity profile for a particular wavelength falls to zero at the interface opposite the incident interface, as shown in Figure 10. This trend was also seen for single illumination, as discussed in previous work.[20,21]

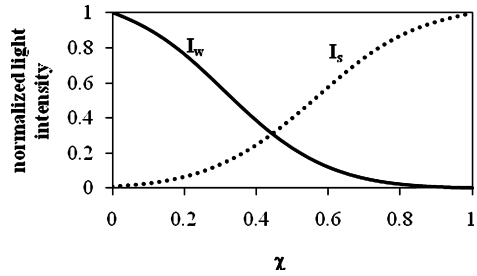

Figure 10. Plots of the light intensity profiles across the membrane under double illumination at optimal transport. For both I_s and I_w, the intensity falls to zero at the interface opposite the incident interface. The carrier is predominantly in the weakly binding form in the dark, and $K^d_s = 5$, $K^d_w = 0.005$, $K_{caro} = 500$, $\varepsilon_{caro} = \varepsilon_{como} = 1$, $\alpha = 50$, $\beta_{car,w} = \beta_{car,s} = \beta_{com,w} = \beta_{com,s} = 10$, and $\varepsilon_s = \varepsilon_w = 0.01$.

Results for Simulations in Which the Carrier Is Predominantly in the Strongly Binding Form in the Dark. The results of simulations of membrane transport for carriers that are primarily in the strongly binding form in the dark are very similar to the results for membranes containing carriers that are primarily in the weakly binding form in the dark. This is not surprising since the values of K_{caro} and K_{como} had no impact on solute flux for double illumination. Hence, solute flux under double illumination should be the same whether the carrier is predominantly in the weakly or strongly binding form in the dark. The only differences are in the efficacy of photopumping under single illumination, but the general trends noted in the previous section also hold true for this set of simulations. Under almost all conditions, double illumination produces significantly greater flux at higher concentration gradients than does single illumination. The only exceptions are very low values of α and large values of ε_s and ε_w. In these cases, solute transport falls off rapidly with increasing concentration gradient under both double and single illumination about the same. These trends were noted and explained in the previous section.

The trend in light intensities needed to maintain optimal flux for carriers that are primarily in the strongly binding form in the dark is the same as that seen for carriers primarily in the weakly binding form in the dark. Doubly illuminated liquid membranes need light intensities at the wavelength to convert the strongly binding form of the carrier to the weakly binding form that are 5−10 greater than light intensities for singly illuminated membranes. Light intensity profiles for optimal solute flux follow the same patterns as for carriers that are primarily in the weakly binding form in the dark.

Conclusions

In general, double illumination yielded significantly higher fluxes across the entire range of sweep concentrations. Not only were doubly illuminated fluxes higher than singly illuminated ones, they were more consistent as well, showing less drop off as the sweep concentration was increased. Moreover, there were several instances where the effect of certain parameters could be deemed negligible under double illumination. Specifically, interconversion rates and equilibrium constants between the weakly and the strongly binding forms of the carrier and complex had no effect on double-illumination flux. This allows for a considerably wider range of membrane/carrier combinations for any given solute of interest. Table 2 summarizes the ranges of parameters for optimal photopumping for carriers that are primarily in the weakly binding form in the dark, while Table 3 summarizes the ranges of parameters for optimal photopumping for carriers that are primarily in the strongly binding form in the dark. While it would be very useful to have lists of anticipated transport rates under various conditions, those rates are very dependent on conditions such as membrane thickness, carrier binding constants, interconversion rates, etc. Consequently, such lists would very long. Rather, Tables 2 and 3 allow for selection of potential carriers, and the text for the simulation program is provided in the Supporting Information, so that investigators can determine anticipated transport rates at specific concentration gradients for themselves.

TABLE 2: Ranges of Parameter Values for Optimal Solute Transport against a Concentration Gradient for Carriers Predominantly in the Weakly Binding Form in the Dark

parameter	single illumination	double illumination
K_{car}	large (>50)	does not matter
ε_{car}, ε_{com}	small (≤1)	does not matter
K^d_w	small (<0.01)	small (<0.01)
K^d_s	moderate (5−10)	moderate (5−10)
α	large (≥50)	large (≥50)
β	large (≥10)	large (≥10)
ε_s, ε_w	small (<0.1)	small (<0.1)

TABLE 3: Ranges of Parameter Values for Optimal Solute Transport against a Concentration Gradient for Carriers Predominantly in the Strongly Binding Form in the Dark

parameter	single illumination	double illumination
K_{car}	moderate (0.1−0.01)	does not matter
ε_{car}, ε_{com}	small (≤1)	does not matter
K^d_w	small (≤0.05)	small (≤0.05)
K^d_s	moderate (5−10)	moderate (5−10)
α	large (≥50)	large (≥50)
β	large (≥10)	large (≥10)
ε_s, ε_w	small (<0.1)	small (<0.1)

The light intensities needed to maintain photopumping under double illumination are also about the same regardless of whether the carrier is predominately in the weakly or strongly binding form in the dark. Light intensity profiles should go to zero at the interface opposite the incident interface for both I_s and I_w. For either type of carrier, significantly higher light intensities are required for optimal photopumping under double illumination than under single illumination. A previous theoretical study of photopumping under single illumination explicitly discussed efficiencies of photopumping in terms of energy stored by creating a concentration gradient versus the energy of the light needed to maintain that concentration gradient.[21] The authors found rather low efficiencies (much less than 0.1%), and doubly illuminated membranes will be much less efficient since they require higher overall light intensities. However, since much higher transport against much higher concentration gradients can be achieved for most carriers under double illumination than under single illumination, the extra photons are likely to be worth it.

Acknowledgment. This work was supported by a grant from the donors of the Petroleum Research Fund, administered by the American Chemical Society (#34578-GB7).

Supporting Information Available: List of equations solved in the simulations and a copy of the text for the FORTRAN program used to solve the equations. This material is available free of charge via the Internet at http://pubs.acs.org.

References and Notes

(1) Mohapatra, P. K.; Manchanda, V. K. Liquid Membrane-Based Separations of Actinides. In *Handbook of Membrane Separations*; Pabby,

A. K., Rizvi, S. S. H., Sastre, A. M., Eds.; CRC Press: Boca Raton, FL, 2009; pp 883−917.

(2) Noble, R. D.; Koval, C. A. Review of Facilitated Transport Membranes. In *Materials Science of Membranes for Gas and Vapor Separation*; Yampolskii, Y., Pinnau, I., Freeman, B., Eds.; John Wiley and Sons: Chichester, England, 2006; pp 411−435.

(3) Yang, X. J.; Fane, A. G.; Soldenhoff, K. *Ind. Eng. Chem. Res.* **2003**, *42*, 392.

(4) Lamb, J. D.; Christenson, M. D. *J. Inclusion Phenom. Mol. Recognit. Chem.* **1998**, *32*, 107.

(5) Noble, R. D.; Koval, C. A.; Pellegrino, J. J. *Chem. Eng. Prog.* **1989**, 58.

(6) Kemena, L. L.; Noble, R. D.; Kemp, N. J. *J. Membr. Sci.* **1983**, *15*, 259.

(7) Schultz, J. S. *Science* **1977**, 197.

(8) Shinkai, S.; Nakaji, T.; Ogawa, T.; Shigematsu, K.; Manabe, O. *J. Am. Chem. Soc.* **1981**, *103*, 111.

(9) Shinkai, S.; Shigematsu, K.; Kusano, Y.; Manabe, O. *J. Chem. Soc., Perkin Trans. 1* **1981**, 3279.

(10) Shinkai, S.; Minami, T.; Kusano, Y.; Manabe, O. *J. Am. Chem. Soc.* **1982**, *104*, 1967.

(11) Sasaki, H.; Ueno, A.; Osa, T. *Chem. Lett.* **1986**, 1785.

(12) Shinkai, S.; Miyazaki, K.; Manabe, O. *J. Chem. Soc., Perkin Trans. I* **1987**, 449.

(13) Goyette, M. L.; Longin, T. L.; Noble, R. D.; Koval, C. A. *J. Membr. Sci.* **2003**, *212*, 225.

(14) Shimidzu, T.; Yoshikawa, M. *J. Membr. Sci.* **1983**, *13*, 1.

(15) Young, R. C.; Feldberg, S. W. *Biophys. J.* **1979**, *27*, 237.

(16) Jain, R.; Schultz, J. S. *J. Membr. Sci.* **1986**, *26*, 313.

(17) Haberfield, P. *J. Am. Chem. Soc.* **1987**, *109*, 6178.

(18) Sasaki, H.; Ueno, A.; Osa, T. *Bull. Chem. Soc. Jpn.* **1988**, *61*, 2321.

(19) Ino, M.; Otsuki, J.; Araki, K.; Seno, M. *J. Membr. Sci.* **1994**, *89*, 101.

(20) Longin, T. L.; Koval, C. A.; Noble, R. D. *J. Phys. Chem. B* **1997**, *101*, 7172.

(21) Longin, T. L.; Koval, C. A.; Noble, R. D. *J. Phys. Chem. B* **1998**, *102*, 2064.

(22) Shinkai, S.; Shigematsu, K.; Sato, M.; Manabe, O. *J. Chem. Soc., Perkin Trans. 1* **1982**, 2735.

(23) Irie, M.; Kato, M. *J. Am. Chem. Soc.* **1985**, *107*, 1024.

(24) Sakamoto, H.; Takagaki, H.; Nakamura, M.; Kimura, K. *Anal. Chem.* **2005**, *77*, 1999.

(25) Longin, T. L.; Fraterman, T.; Nguyen, P. *J. Phys. Chem. B* **2005**, *109*, 21063.

(26) Ruckenstein, E.; Sasidhar, V. *J. Membr. Sci.* **1982**, *12*, 27.

(27) Smith, D. R.; Lander, R. J.; Quinn, J. A. In *Recent Developments in Separation Science*; Li, N. D., Ed; CRC Press: Cleveland, OH, 1977; p 2.

JP106802Q